Spectral-Domain Analysis of Harmonic Effects in Superconducting Quasiparticle Mixers

STAFFORD WITHINGTON AND ERIK L. KOLLBERG, SENIOR MEMBER, IEEE

Abstract—**An algorithm has been developed for calculating the harmonic performance of superconducting quasiparticle millimeter-wave mixers. The scheme uses harmonic balance to determine the steady-state waveform of the large-amplitude voltage which is induced across the tunnel junction by the local oscillator source. A key feature of the new algorithm is that the large-signal tunneling-current calculations are done in the frequency domain rather than in the time domain, and this approach leads to numerically efficient computer simulations. The superiority of the spectral-domain method is particularly pronounced when modeling mixers which incorporate high-quality tunnel junctions with very sharp dc nonlinearities. A simplified mixer simulation has been performed to determine the range of ωCR products for which harmonic effects are likely to be important. An ωCR product of between 3 and 4 appears to be a good compromise between being able to tune out the capacitive reactance at the signal frequency and avoiding the deleterious effects of inadvertent harmonic pumping.**

I. Introduction

THE OPERATION of a superconducting quasiparticle mixer can be modeled by using the quantum theory of mixing developed by Tucker [1]. This theory predicts that a mixer will cease to behave classically when the voltage width of the dc nonlinearity is smaller than or comparable with the photon energy $\hbar\omega/e$ of the incident radiation. The transition from classical to quantum behavior has some remarkable consequences, including the appearance of quantum-limited noise temperatures $\hbar\omega/k$ and conversion gain [2], both of which have been seen experimentally [3]–[5]. A comprehensive review of Tucker's quantum theory of mixing and its experimental verification has been published recently [6].

In almost every case the quantum theory of mixing has been applied by assuming that the large-signal local oscillator voltage appearing across the junction is sinusoidal, or equivalently that the capacitance C of the junction shorts out harmonic currents. This idealization allows the equations describing the mixing process to be expressed in a relatively simple form. However, the simplified version of the theory is only applicable provided that the susceptance ωC of the tunnel junction is several times that of the normal-state conductance $1/R$. There is considerable experimental evidence [7], in the form of unexpectedly low conversion efficiencies and high noise temperatures, that harmonic effects are important for ωCR products of less than about 4. Conversely, there are complications associated with using junctions having ωCR products much greater than 4, because the capacitive reactance must be neutralized at the signal frequency; yet it is difficult to construct broad-band matching networks at millimeter wavelengths. If the full potential of the quasiparticle mixer is to be realized, then a theoretical technique is required whereby the harmonic effects which occur in low-capacitance tunnel-junction mixers can be analyzed. Further motivation for developing such a technique comes from the need to model subharmonically pumped mixers [8].

This paper presents an algorithm for calculating the harmonic performance of superconducting quasiparticle mixers. The scheme uses harmonic balance [9] to determine the steady-state waveform of the large-amplitude voltage induced across the tunnel junction by the local oscillator source. A key feature of the algorithm presented in this paper is that the large-signal tunneling-current calculations are done in the frequency domain. This approach is in contrast to the work of Hicks, Feldman, and Kerr [10], where the calculations were done in the time domain. The spectral-domain method is considerably faster when implemented as a computer program, especially when modeling mixers which incorporate high-quality tunnel junctions having very sharp dc nonlinearities.

II. Large-Signal Analysis

A. The Mixer Circuit

Fig. 1 shows an equivalent circuit which is suitable for analyzing the response of a superconducting tunnel junction when it is excited by a large-amplitude local oscillator voltage. The voltage generator and its series impedance represent the local oscillator source referenced to the electrodes of the tunnel junction, and the parallel impedance takes account of the geometric capacitance of the tunnel

Manuscript received March 21, 1988; revised July 15, 1988. This work was supported by the Royal Society.

S. Withington was with the Department of Radio and Space Science, Chalmers University of Technology, Göteborg, Sweden. He is now with the Cavendish Laboratory, University of Cambridge, Cambridge, CB3 0HE England.

E. Kollberg is with the Department of Radio and Space Science, Chalmers University of Technology, S-412 96 Göteborg, Sweden.

IEEE Log Number 8824268.

0018-9480/89/0100-0231$01.00 ©1989 IEEE

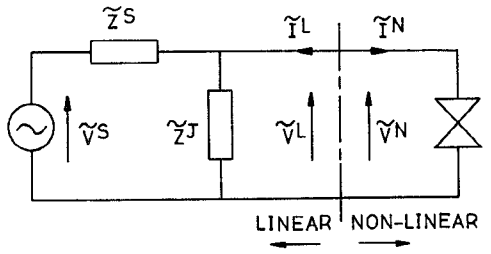

Fig. 1. A large-signal equivalent circuit of a superconducting quasiparticle mixer.

barrier. This simple circuit adequately reflects the principal features of quasiparticle mixers while limiting the complexity of the large-signal analysis; consequently it is suitable for introductory simulations. However, it may be desirable when modeling actual mixers to consider more elaborate embedding networks and these analyses can easily be done by extending the basic method described below.

The voltage source shown in Fig. 1 is assumed to be sinusoidal with an angular frequency ω. This source induces periodic potentials throughout the circuit but in general these are not sinusoidal owing to the influence of the nonlinear tunnel barrier. In the steady state, the various voltages and currents can be expanded as Fourier series having the generic form

$$\begin{bmatrix} v(t) \\ i(t) \end{bmatrix} = \frac{1}{2} \sum_{p=-\infty}^{+\infty} \begin{bmatrix} V_g \tilde{V}_p \\ I_g \tilde{I}_p \end{bmatrix} e^{jp\omega t}. \tag{1}$$

Particular variables are identified by attaching superscripts to the Fourier coefficients, and normalization is denoted by a tilde. For example in Fig. 1, $\tilde{V}^S$ is a vector whose elements $\tilde{V}_p^S$ ($p = 0, \pm 1, \pm 2, \cdots$) are the Fourier coefficients of the normalized local oscillator voltage. Similarly, $\tilde{Z}^S$ is a vector whose elements $\tilde{Z}_p^S$ ($p = 0, \pm 1, \pm 2, \cdots$) are the normalized harmonic impedances of the local oscillator source. A variable with its subscript missing is a vector representing a number of harmonic frequencies. In this paper, all of the electrical quantities are normalized to the dc characteristic of the tunnel junction. The circuit voltages are scaled to a bias voltage V_g which is arbitrarily chosen close to the energy gap, and the circuit currents are scaled to the current I_g which would flow as a result of V_g being applied to the normal-state resistance of the junction ($I_g = V_g/R$). For convenience, these reference quantities can be called the *gap voltage* and the *gap current*, but they do not have any particular physical significance. One advantage of normalizing the voltages and currents in this way is that the circuit impedances become normalized to the normal-state resistance of the junction. Hence it is possible to analyze the performances of actual mixers with only a limited number of standard numerical models.

B. The Harmonic Balance Procedure

The first step in analyzing a mixer circuit is to determine the steady-state waveform of the large-amplitude voltage $\tilde{V}^N$ induced across the tunnel junction by the local oscillator. Once this information is known it is possible to calculate the small-signal admittance matrix. Determining the vector $\tilde{V}^N$ is in general a difficult nonlinear problem because it is necessary to search for a solution which simultaneously satisfies the circuit equations at every harmonic frequency. Various harmonic balance techniques have been devised for handling this type of problem [11] but the relaxation method of Hicks and Khan [12], [13] is particularly easy to realize and therefore it is the one used here.

To implement the procedure, it is first necessary to partition the circuit into two subnetworks, one containing the linear embedding circuit and the other the nonlinear tunnel junction. The harmonic relaxation method is an iterative process which in one form seeks to match the Fourier components of the voltages, across the branch connecting the two subnetworks, on either side of the partition. These are termed the *linear voltage* $\tilde{V}^L$ and the *nonlinear voltage* $\tilde{V}^N$, and they must be equal when a satisfactory solution has been found. It is convenient to replace the local oscillator voltage source and the linear embedding network with a Thévenin source which has an open-circuit voltage of

$$\tilde{V}^T = \frac{\tilde{V}^S \tilde{Z}^J}{(\tilde{Z}^S + \tilde{Z}^J)} \tag{2}$$

and an internal impedance of

$$\tilde{Z}^T = \frac{\tilde{Z}^S \tilde{Z}^J}{(\tilde{Z}^S + \tilde{Z}^J)}. \tag{3}$$

The harmonic balance procedure begins by making a rough estimate of the nonlinear voltage $\tilde{V}^N$. This waveform is simply taken to be the open-circuit voltage of the Thévenin source and therefore the first guess is purely sinusoidal. The initial guess can be written

$$(\tilde{V}^N)_1 = \tilde{V}^T \tag{4}$$

where the subscript outside the parentheses identifies the iteration number. The next step is to use this voltage to calculate the associated quasiparticle current $\tilde{I}^N$. Continuity requires that $\tilde{I}^N$ be equal to the current following out of the linear embedding network $-\tilde{I}^L$; consequently the associated linear voltage is given by

$$(\tilde{V}^L)_1 = \tilde{V}^T - (\tilde{I}^N)_1 \tilde{Z}^T. \tag{5}$$

$(\tilde{V}^L)_1$ can then be compared with $(\tilde{V}^N)_1$ to see if a valid solution has been found. At this early stage they are generally not equal and the nonlinear voltage is reestimated by using

$$(\tilde{V}^N)_{k+1} = P(\tilde{V}^L)_k + (1-P)(\tilde{V}^N)_k, \qquad 0 < P \leq 1 \tag{6}$$

where P is a convergence parameter. The whole procedure is then repeated until a self-consistent solution is found or until a predefined number of iterations have been executed.

The voltage-update method has been chosen in preference to the current-update method for two reasons. First, Tucker's theory allows the tunneling current to be calculated directly from the impressed voltage but the current-

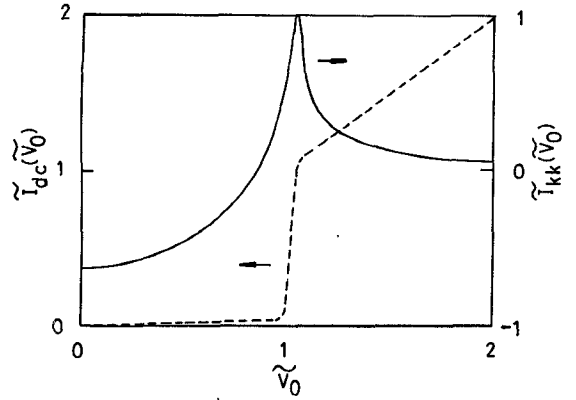

Fig. 2. The normalized dc characteristic $\tilde{I}_{dc}(\tilde{V}_0)$ of a Nb/AlOx/Nb tunnel junction. The Kramers–Kronig transform $\tilde{I}_{kk}(\tilde{V}_0)$ of this function is also shown.

update method requires the current to be the independent variable. Second, the impedances presented to the tunnel barrier at high harmonic frequencies are dominated by the capacitance of the junction, and therefore they are close to being short circuits. When this is the case, the voltage-update method converges faster than the current-update method. An assessment of the convergence properties of the two closely related schemes can be found in the original work of Hicks and Khan [12].

C. Time-Domain Analysis

The harmonic balance procedure requires that the periodic quasiparticle current can be calculated from the periodic voltage appearing across the junction. It will be shown below that it is numerically inefficient to do this calculation in the time domain.

A quasiparticle tunnel junction is characterized in the time domain by a response function $\tilde{\psi}(t)$ [14] which has the normalized form

$$\tilde{\psi}(t) = \frac{j}{\pi}\int_{-\infty}^{+\infty}\left[\tilde{I}_{dc}\left(\frac{\omega'}{\omega_g}\right) - \frac{\omega'}{\omega_g}\right]e^{-j\omega' t}d\omega' \qquad (7)$$

where ω_g is the angular frequency associated with the normalizing gap voltage ($\omega_g = eV_g/\hbar$), and $\tilde{I}_{dc}(\tilde{V}_0)$ is the normalized dc characteristic of the tunnel barrier. For example, Fig. 2 shows the normalized characteristic of a Nb/AlOx/Nb junction [15]. A perfect device with an infinitely sharp nonlinearity has a response function $\psi'(t)$ which oscillates at the gap frequency. Furthermore, the amplitude of $\tilde{\psi}'(t)$ falls off inversely with time at large times. The instantaneous tunneling current is therefore influenced by the voltage which existed across the junction at very long times in the past. However, a real junction has a nonlinearity which is smeared over a finite voltage range, and the question arises as to how far into the past the voltage must be considered when calculating the tunneling current. Insight into this question can be gained by multiplying the response function of the perfect barrier by a Gaussian function having a half-width of Δt, giving

$$\tilde{\psi}(t) = \tilde{\psi}'(t)e^{-(t/\Delta t)^2}. \qquad (8)$$

Equation 7 suggests that, to a first approximation, the dc characteristic associated with the modified response function is effectively the ideal dc characteristic convolved with the Fourier transform of the modifying function, and this transform is a Gaussian having a half-width $\Delta\omega'$ of $2/\Delta t$. The effect of the convolution is to smear out the infinitely sharp nonlinearity. Hence, the voltage width $\Delta\tilde{V}_{dc}$ of the transition region becomes approximately $1/\Delta t f_g$, where f_g is the gap frequency. This last expression has been derived by truncating the Gaussian, with which the ideal dc characteristic is convolved, at the 5 percent level. The number N of gap frequency cycles into the past for which the response function must be considered is $1.7\Delta\tilde{V}_{dc}$, where the time-domain Gaussian has also been truncated at the 5 percent level in order to prevent spurious effects due to Gibb's phenomena. For example, a lead alloy junction may have a $\Delta\tilde{V}_{dc}$ of typically 0.15; therefore 12 cycles of its response function are sufficient to represent the junction. If each cycle is sampled at ten points, then a 120 point analysis is required in order to calculate the tunneling current at a single instant in time. A niobium junction may have a $\Delta\tilde{V}_{dc}$ of typically 0.03; consequently 57 cycles of its response function must be considered, and if each is sampled at ten points then a 570 point analysis is required for every tunneling current calculation. It is evident from this discussion that the computing time required for a single harmonic balance iteration increases dramatically as the quality of the junction is improved.

D. Frequency-Domain Analysis

It will now be shown how the quasiparticle current can be calculated very much more efficiently in the frequency domain. The periodic voltage appearing across the junction modulates the quasiparticle energy eigenstates on one side of the barrier by the phase factor

$$f(t) = e^{-j\omega_g\int_{-\infty}^{t}[\tilde{v}^N(t')-\tilde{V}_0]dt'} \qquad (9)$$

where the effect of the dc bias voltage $\tilde{V}_0$ is removed. This phase factor can be represented in the spectral domain by the Fourier transform

$$W(\omega') = \frac{1}{2\pi}\int_{-\infty}^{+\infty} f(t)e^{j\omega' t}dt. \qquad (10)$$

Moreover, the steady-state voltage across the junction is periodic, and therefore it can be written

$$\tilde{v}^N(t') = \tilde{V}_0 + \sum_{p=1}^{\infty}|\tilde{V}_p^N|\cos(p\omega t' + \phi_p) \qquad (11)$$

where $\phi_p = \angle\tilde{V}_p^N$ and $\tilde{V}_0 = \tilde{V}_0^N/2$. The phase factor which results from this modulation is found by substituting (11) into (9), giving

$$f(t) = e^{-j\sum_{p=1}^{\infty}\alpha_p\sin(p\omega t+\phi_p)} \qquad (12)$$

where

$$\alpha_p = \frac{\omega_g|\tilde{V}_p^N|}{p\omega} = \frac{|\tilde{V}_p^N|}{\tilde{V}_p^{PH}} \qquad (13)$$

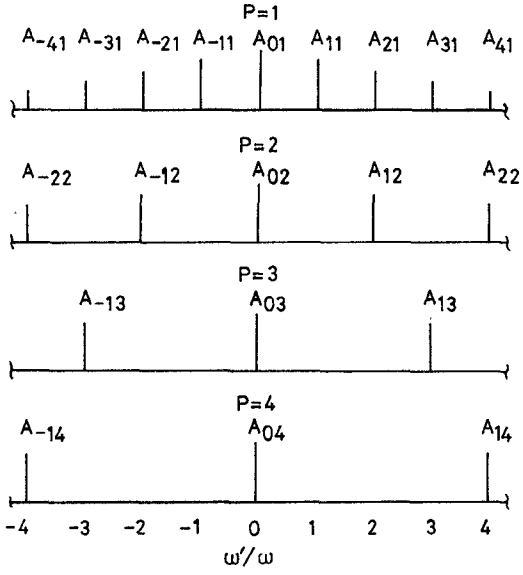

Fig. 3. The spectra $W_P(\omega')$ of the phase factors associated with the first four harmonics of the periodic large-signal terminal voltage.

and $\tilde{V}_p^{\mathrm{PH}}$ is the normalized photon voltage of the pth harmonic. Similarly, it is convenient to use

$$\alpha_s = \frac{\omega_g |\tilde{V}_1^S|}{\omega} \tag{14}$$

for the local oscillator source voltage. By using the Jacobi–Anger equality, (12) can be written in the form

$$f(t) = \prod_{p=1}^{\infty} \sum_{n=-\infty}^{+\infty} A_{np} e^{-jnp\omega t} \tag{15}$$

where the complex coefficients are given by

$$A_{np} = J_n(\alpha_p) e^{-jn\phi_p}. \tag{16}$$

Expanding (15) and retaining only the first J harmonics leads to

$$f(t) = \prod_{p=1}^{J} g_p(t) \tag{17}$$

where

$$g_p(t) = \sum_{n=-\infty}^{+\infty} A_{np} e^{-jnp\omega t}. \tag{18}$$

The function $g_p(t)$ represents the influence of the pth harmonic on the overall phase factor, and the spectrum $W_p(\omega')$ of this contribution is found by substituting (18) in to (10), giving

$$W_p(\omega') = \sum_{n=-\infty}^{+\infty} A_{np} \delta(\omega' - np\omega). \tag{19}$$

The spectra associated with the first four harmonics are shown schematically in Fig. 3. Multiplication in the time domain is equivalent to convolution in the frequency domain; therefore the spectrum of the overall phase factor becomes

$$W(\omega') = W_1(\omega') * W_2(\omega') \cdots W_J(\omega') \tag{20}$$

where the asterisk denotes convolution.

For example, suppose that the voltage across the junction consists of only the fundamental and the second harmonic. The spectrum of the overall phase factor becomes

$$W(\omega') = \int_{-\infty}^{+\infty} W_1(u) W_2(\omega' - u)\, du \tag{21}$$

where

$$W_1(u) = \sum_{n=-\infty}^{+\infty} A_{n1} \delta(u - n\omega) \tag{22}$$

and

$$W_2(\omega' - u) = \sum_{n=-\infty}^{+\infty} A_{m2} \delta(\omega' - u - 2m\omega). \tag{23}$$

Assuming that the resulting spectrum has the form

$$W(\omega') = \sum_{k=-\infty}^{+\infty} C_k \delta(\omega' - k\omega) \tag{24}$$

it can be shown that

$$C_k^2 = \sum_{m=-\infty}^{+\infty} A_{(k-2m)1} A_{m2} \tag{25}$$

where the superscript identifies the number of frequencies involved. This scheme can be extended by convolving into the spectrum the effects of higher harmonics, and this leads to

$$C_k^J = \sum_{m=-\infty}^{+\infty} C_{(k-Jm)}^{(J-1)} A_{mJ} \tag{26}$$

for J harmonics. Finally, the spectrum of the overall phase factor is found by substituting (26) into (24).

The quasiparticle current which tunnels through the barrier in response to this modulation can be calculated by using Werthamer's relationship [16]:

$$\langle \tilde{I}(t) \rangle = \mathrm{Im} \int_{-\infty}^{+\infty} \int_{-\infty}^{+\infty} W(\omega') W^*(\omega'') \cdot e^{-j(\omega' - \omega'')t} \tilde{I}\left(\tilde{V}_0 + \frac{\omega'}{\omega_g} \right) d\omega' d\omega'' \tag{27}$$

where the junction is characterized by the function

$$\tilde{I}(\tilde{V}_0) = \tilde{I}_{kk}(\tilde{V}_0) + j\tilde{I}_{\mathrm{dc}}(\tilde{V}_0). \tag{28}$$

The imaginary part of this expression, $\tilde{I}_{\mathrm{dc}}(\tilde{V}_0)$, is the normalized dc characteristic of the tunnel barrier, and the real part, $\tilde{I}_{kk}(\tilde{V}_0)$, is the Kramers–Kronig transform of the imaginary part, or

$$\tilde{I}_{kk}(\tilde{V}_0) = \frac{1}{\pi} P \int_{-\infty}^{+\infty} \frac{\tilde{I}_{\mathrm{dc}}(\tilde{V}_0') - \tilde{V}_0'}{(\tilde{V}_0' - \tilde{V}_0)} d\tilde{V}_0' \tag{29}$$

where P denotes the Cauchy principal value. The response function of a typical Nb/AlOx/Nb junction is shown in Fig. 2. The tunneling current is determined by substituting the spectrum given by (24) into Werthamer's expression, and this leads to

$$\langle \tilde{I}(t) \rangle = \mathrm{Im} \sum_{p=-\infty}^{+\infty} e^{jp\omega t} \left(\tilde{R}_p + j\tilde{S}_p \right) \tag{30}$$

where

$$\left(\tilde{R}_p + j\tilde{S}_p\right) = \sum_{k=-\infty}^{+\infty} C_k C^*_{p+k} \tilde{I}\left(\tilde{V}_0 + k\tilde{V}_1^{\mathrm{PH}}\right). \quad (31)$$

Comparing this expression with (1) shows that

$$\tilde{I}_p^N = \left(\tilde{S}_p + \tilde{S}_{-p}\right) - j\left(\tilde{R}_p - \tilde{R}_{-p}\right). \quad (32)$$

Therefore, the Fourier components of the tunneling current can easily be calculated once the spectrum of the overall phase factor is known.

III. Small-Signal Analysis

The conversion efficiency of a mixer can easily be calculated once the steady-state phase factor associated with the local oscillator drive has been determined. The nature of this calculation has been considered in some detail by Tucker [1], and the following summary consists of his equations presented in a slightly modified form.

The small-signal sideband voltages and currents can be conveniently represented by the series

$$\begin{bmatrix} v^{SG}(t) \\ i^{SG}(t) \end{bmatrix} = \mathrm{Re} \sum_{m=-\infty}^{+\infty} \begin{bmatrix} V_g \tilde{V}_m^{SG} \\ I_g \tilde{I}_m^{SG} \end{bmatrix} e^{j\omega_m t} \quad (33)$$

where $\omega_m = m\omega + \omega_0$, and ω_0 is the angular intermediate frequency. The sideband voltages and currents are linearly related, for small signals, through the expression

$$\tilde{I}_m^{SG} = \sum_{m'} \tilde{Y}_{mm'} \tilde{V}_{m'}^{SG} \quad (34)$$

where $\tilde{Y}$ is an admittance matrix which is normalized to the normal-state admittance of the tunnel junction. The elements of the matrix are given by (compare with [1, eq. 7.5])

$$\begin{aligned} \tilde{Y}_{mm'} = {} & \frac{-j}{2\left(m'\tilde{V}_1^{\mathrm{PH}} + \tilde{V}^{\mathrm{IF}}\right)} \sum_{n=-\infty}^{+\infty} \sum_{n'=-\infty}^{+\infty} C_n C^*_{n'} \delta_{m-m',n'-n} \\ & \cdot \left[\tilde{I}\left(\tilde{V}_0 + n\tilde{V}_1^{\mathrm{PH}}\right) - \tilde{I}\left(\tilde{V}_0 + (n-m')\tilde{V}_1^{\mathrm{PH}} - \tilde{V}^{\mathrm{IF}}\right)\right. \\ & \left. - \tilde{I}^*\left(\tilde{V}_0 + (n'+m')\tilde{V}_1^{\mathrm{PH}} + \tilde{V}^{\mathrm{IF}}\right) + \tilde{I}^*\left(\tilde{V}_0 + n'\tilde{V}_1^{\mathrm{PH}}\right)\right] \end{aligned} \quad (35)$$

where $\tilde{V}^{\mathrm{IF}}$ is the normalized IF photon voltage $\hbar\omega_0/eVg$ and the C coefficients are those of the steady-state local oscillator phase factor. The IF photon voltage is usually smaller than the voltage scale of the dc nonlinearity, and therefore the output frequency may be treated classically. Expanding the response function to the lowest order about the bias and photon points leads to

$$\begin{aligned} \tilde{Y}_{mm'} = {} & \frac{-j}{2\left(m'\tilde{V}_1^{\mathrm{PH}} + \tilde{V}^{\mathrm{IF}}\right)} \\ & \cdot \sum_{n=-\infty}^{+\infty} \left\{\left[C_n C^*_{m-m'+n} - C_{n+m'} C^*_{n+m}\right]\tilde{I}(n)\right. \\ & + \left[C_{n-m+m'} C_n^* - C_{n-m} C^*_{n-m'}\right]\tilde{I}^*(n) \\ & \left. + \tilde{V}^{\mathrm{IF}}\left[C_{n+m'} C^*_{n+m}\tilde{I}'(n) - C_{n-m} C^*_{n-m'}\tilde{I}'^*(n)\right]\right\} \end{aligned} \quad (36)$$

where the result has been manipulated into a form suitable for computing, and the notation has been simplified by introducing

$$\tilde{I}(n) = \tilde{I}\left(\tilde{V}_0 + n\tilde{V}_1^{\mathrm{PH}}\right) \quad (37)$$

and

$$\tilde{I}'(n) = \frac{\partial}{\partial \tilde{V}_0}\left[I\left(\tilde{V}_0 + n\tilde{V}_1^{\mathrm{PH}}\right)\right]. \quad (38)$$

The admittance matrix can be regarded as representing a multifrequency multiport network which has one port for every sideband. The parallel connection of the junction and the embedding circuit is described by an augmented admittance matrix which can be inverted to give the impedance matrix

$$\|\tilde{Z}_{mm'}\| = \|\tilde{Y}_{mm'} + \tilde{Y}_m^E \delta_{m,m'}\|^{-1} \quad (39)$$

where it is assumed that each sideband is terminated with an admittance $\tilde{Y}_m^E$. The conversion gain G from the upper sideband ($m=1$) to the IF output port ($m=0$) is then given by

$$G = 4\,\mathrm{Re}\left(\tilde{Y}_1^E\right)\mathrm{Re}\left(\tilde{Y}_0^E\right)|\tilde{Z}_{01}|^2. \quad (40)$$

In this expression, $\tilde{Y}_1^E$ and $\tilde{Y}_0^E$ are the normalized source and load admittances, respectively.

IV. Mixer Analysis Algorithm

An algorithm has been developed for calculating the harmonic performance of quasiparticle mixers. The algorithm begins by normalizing and interpolating the dc characteristic of the tunnel junction to produce a regularly sampled function covering the voltage range 0 to $2V_g$. A cubic spline routine is used for the interpolation to ensure continuous first and second derivatives. The large-signal current calculations and the small-signal admittance matrix calculations reference the response function at discrete photon points. Consequently, the sampling interval of the processed characteristic determines the frequency resolution of the mixer analysis. The initialization sequence continues by calculating the Kramers–Kronig transform of the interpolated dc curve by numerical integration. The integral of (29) has a singularity at $\tilde{V}_0' = \tilde{V}_0$; therefore to aid computation it is written as

$$\tilde{I}_{kk}\left(\tilde{V}_0\right) = \lim_{r\to\infty} \frac{2}{\pi}\int_r^{\infty} \frac{1}{2}\left[\tilde{G}\left(\tilde{V}_0''\right) + \tilde{G}\left(-\tilde{V}_0''\right)\right] d\tilde{V}_0'' \quad (41)$$

where

$$\tilde{G}\left(\tilde{V}''\right) = \frac{\tilde{I}_{dc}\left(\tilde{V}_0'' + \tilde{V}_0\right) - \tilde{V}_0'' - \tilde{V}_0}{\tilde{V}_0''}. \quad (42)$$

The integrand is the even part of the function $\tilde{G}(\tilde{V}_0'')$, with the new variable $\tilde{V}_0'' = \tilde{V}_0' - \tilde{V}_0$ having its origin at $\tilde{V}_0' = \tilde{V}_0$. Finally, the initialization sequence calculates the derivatives of both the dc curve and its transform. The file created by this procedure contains a tabulated version of the response function defined by (28).

The linear circuit analysis routine begins by establishing the Thévenin equivalent circuit of the local oscillator source referenced to the electrodes of the tunnel junction. The open-circuit voltage of the Thévenin source is then used as an initial estimate of the large-amplitude voltage appearing across the tunnel junction. The actual waveform of this voltage is determined by the nonlinear circuit analysis part of the algorithm.

The harmonic balance procedure starts by calculating the quasiparticle current associated with the initial estimate of the nonlinear voltage $(\tilde{V}^N)_1$. For a general iteration, the quasiparticle current is calculated by first determining the spectra of the phase factors associated with the harmonic components of the exciting voltage. According to (16) and (19), sequences of Bessel functions must be generated. The Bessel functions in each sequence, all with the same argument, have orders which range from some maximum positive integer to the same magnitude negative integer. These sequences can be generated by backward recurrence. An arbitrary guess is initially made at a high-order Bessel function, and then the lower orders are successively calculated by using the recurrence relationship

$$J_{n-1}(\alpha) = \left(\frac{2n}{\alpha}\right) J_n(\alpha) - J_{n+1}(\alpha). \tag{43}$$

The precision of each order is increased in comparison with its generating higher order, but because the initial guess was arbitrary, the lower orders are relatively correct but inaccurate. This problem can be overcome by normalizing the calculated sequence to the sum

$$J_0(\alpha) + 2J_2(\alpha) + 2J_4(\alpha) \cdots 2J_N(\alpha) \tag{44}$$

which should be unity. The recurrence calculation must begin at a sufficiently high order to achieve the required degree of accuracy in the highest order to be used in the spectrum. Hence the optimum starting order depends on how hard the junction is being pumped. For example, if it is assumed that the arguments of the sequences do not exceed 5, then the highest order to be considered is at the very most 9, and it is sufficient to use $J_{16}(\alpha) = 0$ and $J_{15}(\alpha) = 1 \times 10^{-10}$ to start the recurrence calculation. Once the positive orders of the Bessel functions have been obtained, the negative orders are simply given by

$$J_{-n}(\alpha) = (-1)^n J_n(\alpha). \tag{45}$$

The next step towards determining the quasiparticle current is to convolve the spectra of the harmonic phase factors in the manner described by (25) and (26). It is then straightforward to ascertain the quasiparticle current, from the overall phase factor, by using (31) and (32). The harmonic balance routine continues by calculating the linear voltage which results from the quasiparticle current being conducted through the Thévenin source. This voltage is compared with the original estimate of the drive voltage, and convergence is deemed to have occurred when the ratios of the harmonic magnitudes are within ± 0.1 percent of unity and the phases agree to within 0.5°. If convergence has not occurred, then the nonlinear voltage is reestimated by using (6) together with a convergence parameter which is chosen by means of the minimization technique described by Hicks and Khan [9]. The whole harmonic balance procedure is then repeated until a self-consistent solution is found. Finally, the flow of the algorithm is returned to the linear circuit analysis section, where the admittance matrix and the conversion gain are calculated by using (36) to (40).

TABLE I
THE DEFAULT PARAMETERS OF THE SIMULATED MIXER

$\tilde{V}_g$	= 1.0	V_g	= 3.0 mV
$\tilde{V}_1^{PH}$	= 0.125	f	= 90 GHz
$\tilde{V}_0$	= 0.97	V_0	= 2.9 mV
$\tilde{R}$	= 1.0	R	= 50Ω
$\tilde{Z}_1^S$	= 0.5	Z_1^S	= 25Ω
$\tilde{Z}_2^S$	= 10.0	Z_2^S	= 500Ω

V. EXAMPLE

The mixer analysis algorithm described in Section IV has been implemented as a Fortran program on a Microvax II minicomputer, and a number of simulations have been performed to determine the range of ωCR products for which harmonic effects are important. It is convenient, for the purpose of demonstrating the algorithm, to report the results of a simplified simulation which adequately reflects the principal features of the full calculations. Two simplifications have been made in order to simplify the presentation. The first is that only the fundamental and the second harmonic are considered to be present in the junction drive waveform. This is a good approximation for junctions having an ωCR product of greater than about unity. The second is that the harmonic sidebands are assumed to be open circuited even though the harmonic of the local oscillator is terminated with a finite impedance. This situation does not occur in a real mixer and therefore the assumption is somewhat artificial. However, it has the advantage that only the signal, image, and intermediate frequencies are coupled through the admittance matrix, and therefore the complicated mechanism by which the sideband terminations influence the conversion efficiency can be ignored.

The nonlinear circuit analysis part of the algorithm has been used to investigate the waveform of the large-amplitude voltage which appears across the junction of Fig. 2 when it is installed in a mixer circuit having the default characteristics listed in Table I. In general it has been found that the harmonic balance procedure almost always converges in less than 20 iterations as long as a normalized resistive identity element [9] of 0.5 to 1.0 is used. A

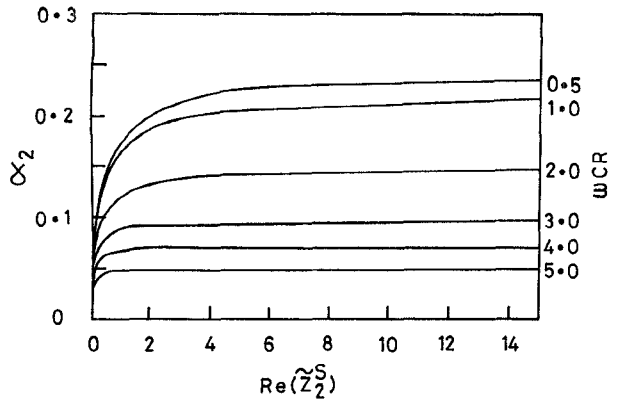

Fig. 4. The magnitude of the second harmonic drive α_2 as a function of the second harmonic embedding resistance $\mathrm{Re}(\tilde{Z}_2^S)$ for parametric values of the ωCR product. The default parameters of the mixer are summarized in Table I, and the response function of the junction is shown in Fig. 2.

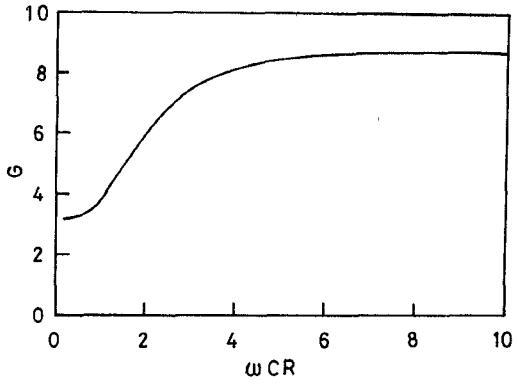

Fig. 5. The conversion gain G as a function of the ωCR product. The default parameters of the mixer are summarized in Table I, and the response function of the junction is shown in Fig. 2. The normalized signal source and load resistances are 0.5 and 0.75, respectively.

complete large- and small-signal analysis usually takes less than 0.5 s, which is considerably faster than can be achieved with a time-domain calculation. The spectral method is markedly superior, even when a greater number of harmonics are included. Fig. 4 shows the magnitude of the second harmonic drive voltage α_2 as a function of the second harmonic embedding resistance $\mathrm{Re}(\tilde{Z}_2^S)$ for parametric values of the ωCR product. The local oscillator source voltage has been held constant at $\alpha_s = 4.0$, which results in $\alpha_1 = 1.4$ for $\omega CR < 4.0$ and $\mathrm{Re}(\tilde{Z}_2^S) = 10$, because this is the drive level which optimizes the conversion efficiency when the mixer is biased in the middle of the first photon step below the gap. Fig. 4 demonstrates that a significant amount of harmonic pumping can occur when the ωCR product is less than about 3; furthermore, it shows that the level of this pumping is relatively independent of the embedding resistance when $\mathrm{Re}(\tilde{Z}_2^S) > 2$.

The conversion gain of the above mixer has been calculated as a function of the ωCR product of the junction, and the results are shown in Fig. 5. The normalized signal source and load resistances were set equal to 0.5 and 0.75, respectively, and the local oscillator source voltage was once again held constant at $\alpha_s = 4.0$. For each value of the ωCR product the junction's capacitive reactance was tuned out at the signal frequency by a parallel susceptance. The conversion gain is significantly reduced for ωCR products of less than about 4. In some simulations the gain begins to rise as the ωCR product is reduced below unity, but this effect has not been studied in any detail. The curve shown in Fig. 5 is characteristic of the results of complete simulations, and it is in agreement with the time-domain calculations of [10] and the experimental data discussed in [7]. It seems that an ωCR product of between 3 and 4 is a good compromise between being able to tune out the capacitance at the signal frequency, and avoiding the deleterious effects of inadvertent harmonic pumping.

VI. Conclusions

An algorithm has been developed for calculating the harmonic performance of superconducting quasiparticle mixers. An iterative harmonic balance procedure is used to determine the waveform of the large-amplitude voltage induced across the tunnel junction by the local oscillator source. During each iteration, the harmonic balance routine must calculate the periodic quasiparticle current which tunnels through the junction when a periodic voltage is applied. It has been demonstrated that it is possible to do this calculation much more efficiently in the frequency domain than in the time domain. The difference in speed is particularly pronounced when modeling mixers which incorporate junctions having very sharp dc nonlinearities. The new algorithm provides, for the first time, an analysis method which is sufficiently fast to enable the harmonic performance of a wide variety of mixer designs to be investigated.

A simplified mixer simulation has been performed to determine the range of ωCR products for which internal harmonic pumping is likely to be important. It appears that harmonic effects can significantly reduce the conversion efficiency if the ωCR product of the junction is less than about 4. This is sufficiently low to enable broad-band mixers to be constructed; therefore it is tentatively concluded that the optimum value of the ωCR product is 4. This conclusion is, however, based on a number of specific simulations and it should not be assumed to apply in all cases. Nevertheless, it is a useful guideline which can be applied when the harmonic impedances are unknown.

Acknowledgment

The first author would like to thank Prof. Booth and Prof. Kollberg and all member of the Radio and Space Science Group for their warm hospitality during his year's stay at Chalmers University of Technology, Sweden. He is most grateful to Dr. Hills of Cambridge University, England, for encouraging the visit.

References

[1] J. R. Tucker, "Quantum limited detection in tunnel junction mixers," *IEEE J. Quantum Electron.*, vol. QE-15, pp. 1234–1258, 1979.

[2] J. R. Tucker, "Predicted conversion gain in superconductor insulator superconductor quasiparticle mixers," *Appl. Phys. Lett.*, vol. 36, pp. 477–479, 1980.

[3] P. L. Richards, T. -M. Shen, R. E. Harris, and F. L. Lloyd, "Quasiparticle heterodyne mixing in SIS tunnel junctions," *Appl. Phys. Lett.*, vol. 34, pp. 345–347, 1979.

[4] T. -M. Shen, P. L. Richards, R. E. Harris, and F. L. Lloyd, "Conversion gain in mm-wave quasiparticle heterodyne mixers," *Appl. Phys. Lett.*, vol. 36, pp. 777–779, 1980.

[5] S. Rudner, M. J. Feldman, E. Kollberg, and T. Claeson, "The antenna-coupled SIS Quasiparticle array mixer," *IEEE Trans. Magn.*, vol. MAG-17, pp. 690–693, 1981.

[6] J. R. Tucker and M. J. Feldman, "Quantum detection at millimeter wavelengths," *Rev. Mod. Phys.*, vol. 57, pp. 1055–1113, 1985.

[7] M. J. Feldman and S. Rudner, "Mixing with SIS arrays," *Reviews in Infrared and Millimeter Waves*, vol. I, pp. 47–75, 1983.

[8] D. Winkler *et al.*, "A sub-mm wave quasiparticle receiver for 750 GHz," in *Proc. Instrumentation for Submillimetre Spectroscopy, SPIE*, vol. 598, pp. 33–38, 1985.

[9] F. Filicori, "Nonlinear microwave circuit analysis using harmonic balance techniques," in *15th European Microwave Conf. Proc.*, 1985, pp. 1104–1109.

[10] R. G. Hicks, M. J. Feldman, and A. R. Kerr, "A general numerical analysis of the superconducting quasiparticle mixer," *IEEE Trans. Magn.*, vol. MAG-21, pp. 208–211, 1985.

[11] K. S. Kundert and A. Sangiovanni-Vincentelli, "Simulation of nonlinear circuits in the frequency domain," *IEEE Trans. Computer-Aided Design*, vol. CAD-5, pp. 521–535, 1986.

[12] R. G. Hicks and P. J. Khan, "Numerical analysis of nonlinear solid-state device excitation in microwave circuits," *IEEE Trans. Microwave Theory Tech.*, vol. MTT-30, pp. 251–259, 1982.

[13] R. G. Hicks and P. J. Khan, "Numerical technique for determining pumped nonlinear device waveforms," *Electron. Lett.*, vol. 16, pp. 375–376, 1980.

[14] J. R. Tucker, "The quantum response of nonlinear tunnel junctions as detectors and mixers," *Reviews in Infrared and Millimeter Waves*, vol. I, pp. 1–46, 1983.

[15] J. M. Lumley, R E. Somekh, J. E. Evetts, and J. H. James, "High quality all refractory Josephson tunnel junctions for squid applications," *IEEE Trans. Magn.*, vol. MAG-21, pp. 539–542, 1985.

[16] N. R. Werthamer, "Nonlinear self-coupling of Josephson radiation in superconducting tunnel junctions," *Phys. Rev.*, vol. 147, pp. 255–263, 1966.

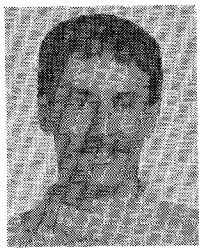

Stafford Withington graduated from the University of Bradford, England, in 1979 with a degree (first class honours) in electrical and electronic engineering. His undergraduate industrial training was done with Rolls-Royce Engines (1971) Ltd, Marconi Space and Defence Systems Ltd, and Thorn Electronics Ltd. In 1983 he was awarded the Ph.D. degree by the University of Manchester, England, for his work at Ferranti Microwave Electronics Ltd. on low-noise microwave amplifiers, and for his work at the Nuffield Radio Astronomy Laboratories, Jodrell Bank, on celestial masers.

Between the years 1982 and 1985 he was at the Cavendish Laboratory, University of Cambridge, England, developing cryogenically cooled microwave and millimeter-wave radiometers. After spending a year with the Radio and Space Science Group, Chalmers University of Technology, Sweden, on a Royal Society Fellowship, he returned to Cambridge to work on superconducting millimeter-wave mixers. During the year 1987 to 1988 he lectured in the Department of Electronic Engineering at the University of Sheffield, England. He is currently at the Cavendish Laboratory, University of Cambridge, developing low-noise microwave and millimeter-wave components and systems.

✠

Erik L. Kollberg (M'83–SM'83) received the M.Sc. degree in 1961 and the Teknologie Dr. degree 1971 from Chalmers University of Technology, Göteborg, Sweden.

He has been a professor at the same university since 1974. Dr. Kollberg has published more than a hundred scientific papers in international journals in the field of maser amplifiers, millimeter-wave Schottky diode mixers, superconducting mixers, GaAs devices, and other subjects related to millimeter-wave techniques. He is responsible for the development of low-noise receivers for the Onsala Space Observatory and the new Swedish-European millimeter wave telescope in Chile.

Dr. Kollberg received the microwave prize at the European Microwave Conference in Helsinki in 1984. He is currently serving as chairman of the Swedish IEEE MTT-S Chapter.